JOURNAL OF GEOPHYSICAL RESEARCH: EARTH SURFACE, VOL. 118, 925–936, doi:10.1002/jgrf.20072, 2013

Dynamics of ice stream temporal variability: Modes, scales, and hysteresis

A. A. Robel,[1] E. DeGiuli,[2,3] C. Schoof,[4] and E. Tziperman[1]

Received 13 November 2012; revised 11 February 2013; accepted 27 March 2013; published 31 May 2013.

[1] Understanding the mechanisms governing temporal variability of ice stream flow remains one of the major barriers to developing accurate models of ice sheet dynamics and ice-climate interactions. Here we analyze a simple model of ice stream hydrology coupled to ice flow dynamics and including drainage and basal cooling processes. Analytic and numerical results from this model indicate that there are two major modes of ice stream behavior: steady-streaming and binge-purge variability. The steady-streaming mode arises from friction-stabilized subglacial meltwater production, which may also activate and interact with subglacial drainage. The binge-purge mode arises from a sufficiently cold environment sustaining successive cycles of thinning-induced basal cooling and stagnation. Low prescribed temperature at the ice surface and weak geothermal heating typically lead to binge-purge behavior, while warm ice surface temperature and strong geothermal heating will tend to produce steady-streaming behavior. Model results indicate that modern Siple Coast ice streams reside in the binge-purge parameter regime near a subcritical Hopf bifurcation to the steady-streaming mode. Numerical experiments exhibit hysteresis in ice stream variability as the surface temperature is varied by several degrees. Our simple model simulates Heinrich event-like variability in a hypothetical Hudson Strait ice stream including dynamically determined purge time scale, till freezing and basal cooling during the binge phase. These findings are an improvement on studies of both modern and paleo-ice stream variability and provide a framework for interpreting complex ice flow models.

Citation: Robel, A. A., E. DeGiuli, C. Schoof, and E. Tziperman (2013), Dynamics of ice stream temporal variability: Modes, scales, and hysteresis, *J. Geophys. Res. Earth Surf.*, *118*, 925–936, doi:10.1002/jgrf.20072.

1. Introduction

[2] Ice streams are regions of ice sheets that flow 2–3 orders of magnitude faster than typical glacial ice and currently account for over 90% of the mass flux from the interior of the Antarctic ice sheet to the margins, although covering less than 5% of its total area [*Bamber et al.*, 2000].

[3] The variability of ice stream flow on time scales of tens to thousands of years plays an important role in determining ice sheet mass balance. Observations indicate that the stagnation of Kamb Ice Stream 150 years ago [*Retzlaff and Bentley*, 1993] may be the primary cause for the currently positive mass balance in West Antarctica [*Joughin and Tulaczyk*, 2002]. Further geological evidence has suggested that other Siple Coast ice streams have exhibited considerable variability in the last 1000 years [*Hulbe and Fahnestock*, 2007; *Catania et al.*, 2012]. The ongoing slowing of Whillans Ice Stream [*Hulbe and Whillans*, 1997] and the possibility of reactivation of Kamb Ice Stream [*Vogel et al*., 2005] suggest that ice stream variability will continue to have a major influence on ice sheet mass balance and global rates of sea level rise over the next several centuries.

[4] The variability of a Hudson Strait ice stream has been implicated as a main factor in Heinrich events, large periodic ice discharge events from the Laurentide ice sheet during the last glacial period [*Heinrich*, 1988]. Current geochemical estimates of Heinrich event characteristics [*Hemming*, 2004] are sufficiently broad to suggest that Heinrich event modeling may be useful in constraining the record. Studies of IRD provenance indicate that Heinrich layers in North Atlantic sediment cores point to Hudson Strait ice stream variability as the ice source [*Hemming*, 2004]. Further geological evidence [*Andrews and Maclean*, 2003] suggests the Hudson Strait ice stream was similar to modern Siple Coast ice streams (although on a much larger scale), indicating that both may share a single mechanism of variability.

Additional supporting information may be found in the online version of this article.

[1]Department of Earth and Planetary Sciences, Harvard University, Cambridge, Massachusetts, USA.
[2]Department of Mathematics, University of British Columbia, Vancouver, British Columbia, Canada.
[3]Now at Center for Soft Matter Research, Department of Physics, New York University, New York, New York, USA.
[4]Department of Earth and Ocean Sciences, University of British Columbia, Vancouver, British Columbia, Canada.

Corresponding author: A. A. Robel, Department of Earth and Planetary Sciences, Harvard University, 20 Oxford Street, Cambridge, MA 02138, USA. (robel@fas.harvard.edu)

2169-9003/13/10.1002/jgrf.20072

[5] Our simple model can be useful as a guide for complex model studies in picking an appropriate parameter regime and constructing a reasonable ice stream geometry. *MacAyeal* [1993] constructed a relaxation oscillator model of the entire Laurentide ice sheet by exploiting its characteristic binge and purge time scales and without explicitly considering the possibility of a Hudson Strait ice stream. *MacAyeal* [1993] was successful in reproducing observed Heinrich event period, but had to assume a characteristic ice stream purge time scale of approximately 250 years. Since our model explicitly simulates ice stream dynamics, we are able to predict key parameters of interest, such as purge time scale, till freeze-on thickness and basal cooling amplitude. *Marshall and Clarke* [1997] explicitly simulate the Laurentide ice sheet and a hypothetical Hudson Strait ice stream using a complex model, but were not able to reproduce discharge within the wide range of proxy records. Other studies [*Calov et al.*, 2002, 2010] have also attempted to reproduce the period and amplitude of Heinrich ice discharge events, but cite the need for evolving drainage and till mechanics in order to gain a full understanding of the physical processes that cause Hudson Strait ice stream variability.

[6] High ice stream velocities are caused by the deformation of meltwater-saturated, weak subglacial till [*Alley et al.*, 1986; *Blankenship et al.*, 1986; *Engelhardt et al.*, 1990]. In Antarctica, this meltwater originates at the ice-bed interface, which is maintained at the pressure-melting point during the active ice stream phase. The resulting weak bottom stress is complemented by lateral stresses at ice stream margins in resisting the weak driving stress typical of Antarctic ice streams [*Echelmeyer et al.*, 1994; *Jackson and Kamb*, 1997]. Changes in the strength of subglacial till shift the balance of resistive stresses and may significantly alter ice stream velocity [*van der Veen and Whillans*, 1996]. Observations also indicate that complex drainage networks exist at the ice-bed interface that may provide a means for transporting locally produced meltwater over long distances [*Engelhardt and Kamb*, 1997; *Winberry et al.*, 2009], significantly complicating the problem of modeling ice stream hydrology and dynamics.

[7] The complexities of ice stream dynamics have been modeled using a diverse array of approaches. *Tulaczyk et al*. [2000b] used a highly reduced model and found that multiple modes of ice stream flow are possible, depending on the subglacial net heat flux and changes in subglacial production of meltwater. Complex models often incorporate parameterizations of observed small scale phenomena, such as drainage networks. Two studies [*Bougamont et al.*, 2003a, 2003b] coupled a flow band model to a simple hydrology model similar to that of *Tulaczyk et al.* [2000b]. Another study [*van der Wel et al.*, 2013] coupled a flow band model to both simple local hydrology and a dynamic drainage model. Similarly, *Bougamont et al*. [2011] coupled a complex Herterich-Blatter-Pattyn ice model [*Herterich*, 1987; *Blatter*, 1995; *Pattyn*, 2002] to a simple hydrology model. This later study found that sustained oscillatory ice stream behavior was not attainable without a seemingly ad hoc supply of water from a parameterized regional drainage network. Related complex model studies of hydrology beneath ice sheets [*Payne*, 1995; *Dunse et al*., 2011; *Van Pelt and Oerlemans*, 2012] have found that multiple distinct modes of ice sheet flow exist depending on the state of the subglacial thermal heat budget. *Sayag and Tziperman* [2009] showed that the spatial structure of ice streams suggests a multivalued sliding law. Prescribing such a law, they then [*Sayag and Tziperman*, 2011] found either oscillatory or steady-streaming modes, depending on the rate of upstream ice supply. However, they did not explicitly include the physics that lead to the prescribed sliding law.

[8] This paper studies the interaction of ice stream dynamics, basal hydrology and thermal processes to understand the physical conditions that may give rise to and modulate ice flow variability on a range of time scales. We build a simple model, described in the next section, to simulate the subglacial heat budget, the resulting production or consumption of meltwater and its impact on till deformation. Our central aim is to explore possible ice stream behaviors and their dependence on physical parameters.

[9] We make a number of key improvements to earlier simple models [*Tulaczyk et al.*, 2000b; *MacAyeal*, 1993] while retaining the simplicity that permits a wide range of parameter experimentation and analytic approaches. In particular, this model allows both ice thickness and meltwater content to vary, providing the essential two degrees of freedom necessary for oscillatory behavior [*Fowler*, 1987; *Fowler et al.*, 2001]. We also allow for the possibility of till freeze-on and basal ice cooling during stagnant intervals of till overconsolidation, altering the subglacial heat flux. If till becomes saturated, drainage is permitted and may have a significant impact on the final equilibrium that would otherwise not be reached in the absence of drainage.

[10] The resulting ice stream flow evolution includes two regimes, a steady-streaming mode and a binge-purge mode. These modes are qualitatively similar to the modes found first by *Payne* [1995] (and later *Sayag and Tziperman*, [2009, 2011]; *Dunse et al.*, [2011]; and *Van Pelt and Oerlemans*, [2012]) with complex ice sheet models. In these latter two studies, subglacial hydrology is parameterized with empirical sliding parameters, which are then varied in order to demonstrate that there are multiple possible modes of ice sheet behavior, including high- and low-frequency cyclicity and steady flow. In this study, we focus on ice stream-like geometry and explicitly simulate till mechanics and the basal heat budget, which obviates the need for either ad hoc parameterizations or poorly constrained empirical sliding laws. The flow mode is determined by the balance between different sources of heating and cooling at the ice-bed interface and meltwater drainage. This provides a general framework to interpret the special cases of other simple and complex model studies in terms of readily measurable physical parameters like geothermal heat flux and ice surface temperature.

[11] Additionally, the nature of the transition between these two modes is not always smooth, taking the form of a subcritical Hopf bifurcation. In short, a supercritical Hopf bifurcation occurs when variation of a parameter causes a system to smoothly change from steady state to an oscillating equilibrium state of infinitesimal amplitude. In a subcritical Hopf bifurcation, variation of a parameter causes a system to change from a steady state to an oscillating equilibrium state of large amplitude [*Strogatz*, 1994]. In our model, the occurrence of this type of bifurcation produces

Table 1. Parameters Used in This Study[a]

Constant	Description	Value
a'	Till empirical coefficient (Pa)	1.41×10^6
a_c	Accumulation rate (m yr^{-1})	0.1
A_g	Glen's law rate factor (Pa^{-3} s^{-1})	5×10^{-25}
b	Till empirical exponent	21.7
C_i	Volumetric heat capacity of ice (J K^{-1} m^{-3})	1.94×10^6
e_c	Till consolidation threshold	0.3
g	Acceleration due to gravity (m s^{-2})	9.81
h_b	Thickness of temperate ice layer (m)	10
k_i	Thermal conductivity of ice (J s^{-1} m^{-1} K^{-1})	2.1
L	Ice stream trunk length (km)	500
L_f	Specific latent heat of ice (J kg^{-1})	3.35×10^5
n	Glen's law exponent	3
W	Ice stream trunk width (km)	40
w_s	Till saturation threshold (m)	1
Z_s	Initial effective till layer thickness (m)	1
ρ_i	Ice density (kg m^{-3})	917
ρ_w	Water density (kg m^{-3})	1000

[a]Unless Otherwise Indicated.

hysteresis in cases that may have important implications for climate-ice stream interactions.

2. Model Description

[12] We model an ice stream as a single lumped spatial element in order to focus on temporal (rather than spatial) evolution. All spatial derivatives are approximated using finite-differencing over the spatial scales of interest. The model domain is a rectangle of length L in the streamwise x-direction, corresponding to the entirety of the ice stream trunk, and width W in the cross stream y-direction, corresponding to ice stream width between shear margins. We assume that $\frac{W}{L} \ll 1$, and that vertical shear contributes negligibly to ice stream velocity. The velocity field in the ice stream is determined by lateral and basal shear stress balancing the driving stress acting on an ice stream cross section. To obtain a spatially lumped model, we then assume that a single velocity can be used to represent ice discharge from the ice stream [*Raymond*, 1996, 2000].

[13] The model describes the rate of meltwater production at the ice-bed interface, which evolves in response to ice and till dynamics, and may activate different physical processes depending on the till state. Section 2.1 describes the ice thickness evolution equation, followed by the meltwater budget in section 2.2, ice sliding velocity in section 2.3 and till and basal ice properties in section 2.4. For values of all constants referenced hereafter and used to generate Figures 1–6 (unless otherwise noted), see Table 1.

2.1. Ice Stream Thickness

[14] Changes in ice stream thickness are the result of a balance between accumulation from snowfall and removal due ice stream velocity. The resultant balance is

$$\frac{\mathrm{d}h}{\mathrm{d}t} = a_c - \frac{u_b h}{L}, \tag{1}$$

where a_c is the constant accumulation rate and u_b is the basal sliding velocity. The second term on the right-hand side of this equation is an approximation of the ice flux, $\frac{\partial}{\partial x}(u_b h)$, assuming that ice thickness vanishes at the downstream boundary and sliding velocity is spatially uniform within the domain. Ice flux from upstream tributaries is assumed to be negligible. Basal melting and freeze-on are small compared to accumulation and ice flux, and so are neglected from this mass balance.

2.2. Meltwater Budget

[15] When the temperature of the bed, T_b, is at the melting point, $T_b = T_m$, the bed can have a non-zero water content w. This is related to the bed void ratio e through $w = eZ_s$, where Z_s is the thickness that unfrozen till would occupy if it were reduced to zero porosity. When $w > 0$, it evolves according to

$$\frac{\mathrm{d}w}{\mathrm{d}t} = m - \frac{Q_d}{LW} \tag{2}$$

where m is basal melt rate and Q_d is the volumetric discharge rate through all subglacial conduits below the ice stream. In this model, w and Z_s are dynamically evolved and $e = \frac{w}{Z_s}$ is calculated diagnostically.

[16] m can be related to geothermal heat flux G, conduction into the ice and heat dissipated by sliding at the bed [as in *Lingle and Brown*, 1987; *Tulaczyk et al.*, 2000b; *Joughin et al.*, 2004]

$$m = \frac{1}{\rho_i L_f}\left[G + \frac{k_i(T_s - T_b)}{h} + \tau_b u_b\right], \tag{3}$$

where T_s is the prescribed ice surface temperature, T_b is the basal temperature, k_i is the thermal conductivity of ice, τ_b is the basal shear stress so that $\tau_b u_b$ represents frictional heating, while ρ_i is the density of glacial ice and L_f is the latent heat of fusion. Negative m corresponds to the freezing of basal water. Vertical ice temperature variations are here assumed to be linear from the basal ice temperature to the prescribed surface temperature. Corrections to this approximation would likely result in a larger vertical temperature gradient near the bed [*Joughin et al.*, 2004].

[17] When w reaches zero from above, both u_b and the frictional heating term in the expression for m are set to zero as all the till is frozen and basal temperature may drop below T_m. Additionally, when $w = 0$, $T_b = T_m$ and $m = G + \frac{k_i(T_s - T_m)}{h} > 0$ then till begins to thaw and $\frac{\mathrm{d}w}{\mathrm{d}t} = m$.

[18] When the till water content exceeds an upper saturation threshold (w_s), we assume that till has become saturated and all additional production of meltwater goes directly into drainage,

$$Q_d = \begin{cases} 0 & \text{if } w < w_s \text{ or } m < 0 \\ mLW & \text{otherwise} \end{cases}. \tag{4}$$

Simulating the evolution of drainage channels over a permeable bed requires model complexity that is significantly beyond the scope of this study. We assume that subglacial drainage will reach steady state on a time scale [days to months; see *Schoof*, 2010] that is short compared to the relaxation time scale of the bed (years), hence, we have neglected this drainage evolution time scale. Incorporating a constant level of excess meltwater drainage from upstream sources would simply shift the location of parameter regimes, and thus it has been neglected in this study.

2.3. Ice Basal Sliding Velocity

[19] We neglect any velocity components due to ice deformation or sliding unrelated to till deformation. Thus, velocity is determined by a balance between driving stress, τ_d and a combination of basal shear stress, τ_b and the lateral stress. In that case, *Raymond* [1996] computes the centerline sliding velocity of an ice stream,

$$u_b = \frac{A_g W^{n+1}}{4^n (n+1) h^n} \max\left[\tau_d - \tau_b, 0\right]^n, \tag{5}$$

where A_g is a constant creep parameter in the shear margins and $\tau_d = \rho_i g \frac{h^2}{L}$ is an approximation of the driving stress with acceleration due to gravity, g. Enforcing a positive sliding velocity in equation (5) arises from the Coulomb friction law, in which there is no sliding when the yield stress of the bed is not attained [*Schoof*, 2006]. For the ice flow geometry assumed, this is the case when the yield stress exceeds driving stress. Although *Raymond* [1996] calculated an expression for u_b which included cross-stream variations, we neglect these in the same fashion as *Tulaczyk et al.* [2000b], since they are small and have a minimal impact on the ice stream flux in equation (1). When drainage is active, τ_b is small and $u_b \propto \left(\frac{\tau_d}{h}\right)^n$.

2.4. Till and Basal Ice Properties

[20] Following *Tulaczyk et al.* [2000a], till strength can be modeled as a Coulomb friction law, $\tau_b = \mu N$, where N is the effective pressure and μ is a friction coefficient. This can be expressed directly in terms of void ratio

$$\tau_b = \begin{cases} a' \exp(-b(e - e_c)) & \text{if } w > 0 \\ \infty & \text{otherwise} \end{cases}, \tag{6}$$

where e_c is a till consolidation threshold, a' is the till strength at e_c (different from a given in *Tulaczyk et al.* [2000a] by a factor of $\exp(be_c)$) and b is also a constant. This assumes that e_c is a lower bound on the void ratio. In this study we only use equation (6) to model till strength as a function of void ratio (hence, we do not need to explicitly specify μ or calculate N).

[21] At low void ratios, the hydraulic processes described previously are no longer expected to be applicable. Once the till becomes sufficiently consolidated and bed strength is sufficiently large, surface tension effects are no longer able to maintain a clean ice-till interface, and a frozen fringe can propagate into the sediment matrix [*Rempel*, 2008]. We assume that this happens at the consolidation threshold, e_c, and that, once the growth of a frozen fringe is initiated, all subsequent freezing will occur inside the till, so that

$$\frac{dZ_s}{dt} = \begin{cases} 0 & \text{if } e > e_c \text{ or } Z_s = 0 \\ \frac{m}{e_c} & \text{if } e = e_c \text{ and } Z_0 > Z_s > 0 \end{cases}, \tag{7}$$

where Z_0 is the maximum sediment thickness available.

[22] Once the till layer has completely frozen ($Z_s = 0$), basal ice may cool down, reducing the vertical ice temperature gradient,

$$\begin{aligned} &T_b = T_m \text{ if } w > 0 \\ &\frac{\mathrm{d}T_b}{\mathrm{d}t} = \frac{\rho_i L_f}{C_i h_b} m \text{ if } w = 0 \text{ and either } (T_b = T_m \text{ and } m < 0) \text{ or } (T_b < T_m) \end{aligned}, \tag{8}$$

where C_i is the heat capacity of ice and h_b is the thickness of the temperate basal ice layer that is being cooled. This serves as an approximation to a fully dynamic model for vertical heat diffusion through an ice stream [*MacAyeal*, 1993].

3. Results

[23] Figure 1 shows four characteristic behaviors exhibited by the ice stream model at different prescribed ice surface temperatures. They can broadly be separated into two categories. Figures 1a and 1b show stable fixed points, where ice stream velocity reaches an equilibrium after some initial transient behavior, via two mechanisms.

[24] In Figure 1a, till water content quickly reaches the saturation threshold, w_s, beyond which drainage removes the excess of meltwater being produced. Ice stream velocity, facilitated by the weak bed also reaches an equilibrium. In this state, a very weak bed coexists with subglacial drainage that removes meltwater as it is produced.

[25] In Figure 1b, the initial rate of meltwater production is insufficient to sustain till layer saturation. Till water content rapidly rises due to a high geothermal flux and low vertical heat conduction. This causes a rise in velocity and therefore thinning of the ice stream. Thinning leads to an increase in vertical heat conduction, until it exceeds the prescribed geothermal heat flux and the additional frictional heating, turning the subglacial heat budget negative. Till water content then drops as meltwater is frozen out of the till, leading to till consolidation and ice stream stagnation. During stagnation, slow ice stream thickening from accumulation decreases vertical heat conduction until the ice stream is reactivated. This repeats with decreasing amplitude as the ice surface temperature is insufficiently low to maintain this cycle. Eventually, the ice stream reaches an equilibrium velocity similar to that of the drained example of Figure 1a. In this case, the equilibrium is maintained by the additional heating due to friction at the bed. This is identical to the "ice stream mode" identified by *Tulaczyk et al.* [2000b], although, in this case, the steady state ice thickness is dynamically determined, rather than prescribed.

[26] Both of these mechanisms (Figures 1a and 1b) result in steady state behavior that is very similar. The primary difference is that one equilibrium permits the sustained existence of a subglacial drainage and the other does not. We refer to both collectively as the "steady-streaming mode." Figures 1c and 1d, on the other hand, show stable limit cycles, where ice stream velocity oscillates indefinitely. The activation of different physical processes in the corresponding two parameter regimes yields oscillations of very different amplitudes and periods.

[27] In Figure 1c, a sufficiently cold ice surface is able to sustain the same cycle of accumulation and purging that led to the damped oscillations seen in Figure 1b. This weak binge-purge mode is qualitatively similar to the binge-purge oscillations of *MacAyeal* [1993]. However, rather than a prescribed purge time scale, as in *MacAyeal* [1993], this ice stream model sets its own time scale.

[28] In Figure 1d, a very cold atmospheric temperature enables long periods of stagnation during which till is completely frozen and basal ice is cooled. When ice thickening due to accumulation and the resulting weakening of the vertical temperature gradient have turned the subglacial heat

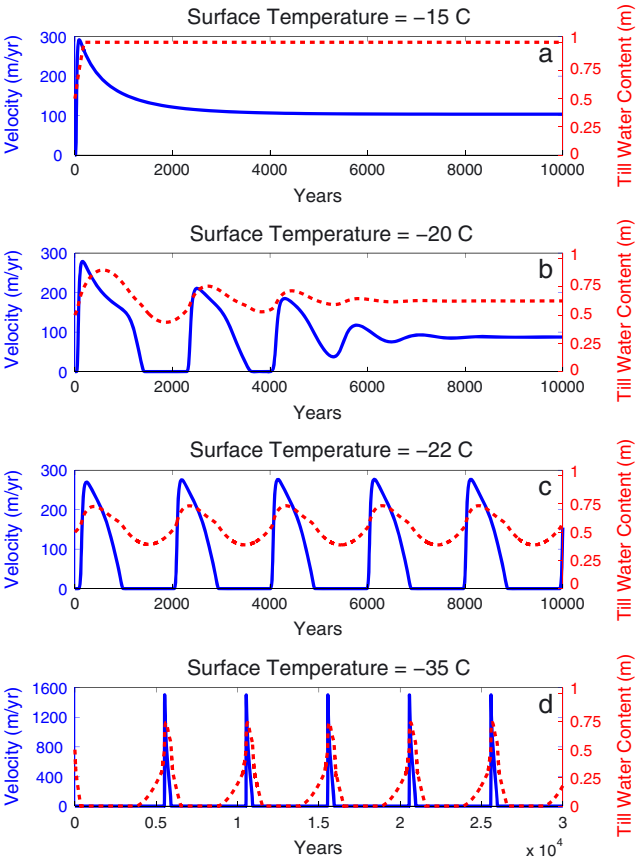

Figure 1. Characteristic numerical results for the ice stream model with parameters given by Table 1, geothermal heat flux of 0.07 Wm^{-2} and four different prescribed surface temperatures (see location in parameter space in Figure 2). In all panels, ice sliding velocity is a blue solid line and till water content is a red dashed line. (a) Steady-streaming with drainage; (b) Steady-streaming without drainage; (c) Weak binge-purge oscillation; (d) Strong binge-purge oscillation.

budget positive, basal ice warms to the pressure-melting point, till is thawed and renewed meltwater production results in ice stream reactivation. The ice stream has thickened significantly during the long stagnant period, leading to high driving stress (compared to typical modern ice streams) that results in a reactivated ice stream velocity that is much higher than in the weak binge-purge mode. We refer to this as the strong binge-purge mode.

[29] The weak and strong binge-purge modes are similar qualitatively. However, it is important to note that the strong binge-purge cycle is enabled by till freezing and basal cooling, which do not occur in the weak case, where stagnation occurs above the till consolidation threshold, e_c due to a weaker negative heat flux (see section 3.4).

[30] Figure 2 is a plot of ice thickness oscillation range as a function of two main parameters: the geothermal heat flux amplitude and ice surface temperature. The four regimes described above represent a transect through the full parameter space of this simple ice stream model (white stars in Figure 2). The steady-streaming mode occurs for warm ice surface temperature and high geothermal heat flux (above solid white lines of Figure 2). At lower ice surface temperatures and geothermal heat flux (below solid white lines of Figure 2), there is an abrupt transition (in the form of a subcritical Hopf bifurcation, see section 3.2) to the weak binge-purge mode. In the region between the two solid white lines of Figure 2, the ice stream may reach either mode, depending on initial conditions of ice thickness and till water content. At yet colder ice surface temperatures and lower geothermal heat flux, there is a stronger binge-purge mode.

[31] Figure 3 is a plot of the period of ice stream oscillations as a function of the same two parameters as in Figure 2. Oscillation period is mostly proportional to oscillation amplitude. Within a robust range of parameters, we find most periods to be of order 10^3 years, reaching a minimum of 800 years. This aligns with other models with thermally induced oscillations [*MacAyeal*, 1993; *Bougamont et al.*, 2003b], but appears to be larger than the ice stream oscillation periods suggested by recent studies of modern Siple Coast ice streams [*Hulbe and Fahnestock*, 2007; *Catania et al.*, 2012].

3.1. Stability Boundary

[32] We set out to determine the location of the stability boundary between the two modes of ice stream behavior.

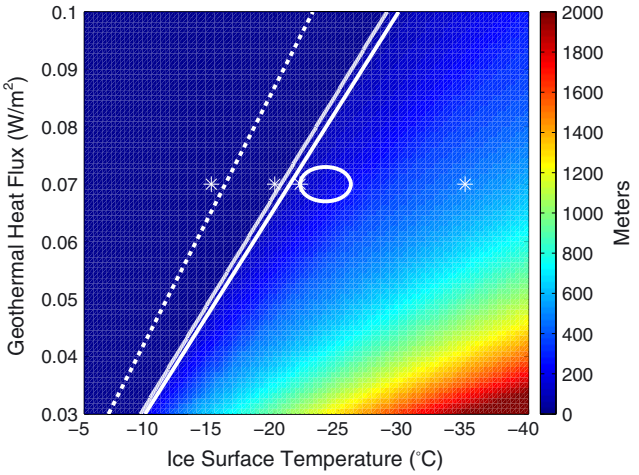

Figure 2. Ice thickness oscillation range (in meters) on a plane of the parameter space for which geothermal flux and ice surface temperature are varied and dimensionless parameter α is constant. Rightmost white solid line is analytic approximation to stability boundary between steady-streaming (zero range region in top-left) and binge-purge (finite range region in bottom-right) modes (accurate to within the thickness of the line). Leftmost white solid line is the location of the last appearance of binge-purge oscillations in numerical simulations. Both solid white lines bound the region of hysteresis. White dashed line is boundary between steady-streaming with and without drainage. White stars indicate locations of characteristic examples plotted in Figure 1. White ellipse marks approximate parameter regime of modern Siple Coast ice streams. Ellipse drawn using geothermal heat flux range estimates cited in [*Joughin et al.*, 2004] and a conservative range of mean air temperatures over Siple Coast ice streams from UWisc AMRC data found at amrc.ssec.wisc.edu/aws/.

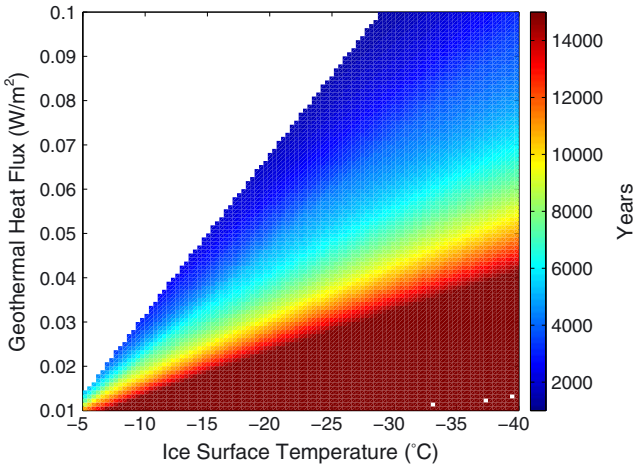

Figure 3. Binge-purge oscillation period (in years) on a plane of the parameter space for which geothermal flux and ice surface temperature are varied and dimensionless parameter α is constant.

The steady-streaming mode corresponds to the steady state solution of our model, and we test for conditions under which this steady state becomes unstable to small perturbations. Such an instability would render the steady-streaming mode unattainable, whereas a stable steady state means that the steady-streaming mode can be realized in practice.

[33] To test for instability, it suffices to consider small departures from the steady state achieved in Figure 1b which does not involve drainage, till freeze-on or basal cooling and is time-independent. This reduces our model to equation (1) and

$$\frac{\mathrm{d}w}{\mathrm{d}t} = m \tag{9}$$

with m calculated from equation (3) and $T_b = T_m$ prescribed. u_b is calculated as before and we define ΔT as the surface temperature departure from T_m. This is similar to the undrained plastic bed model first developed in *Tulaczyk et al.* [2000b], with the key difference being inclusion of dynamically evolving ice thickness (which has also been included in more complex model studies such as *Bougamont et al.* [2003a, 2003b]). Non-dimensionalization of this reduced model yields the following system

$$\frac{\mathrm{d}h^*}{\mathrm{d}t^*} = 1 - h^* u_b^* \tag{10}$$

$$\alpha \frac{\mathrm{d}w^*}{\mathrm{d}t^*} = \tau_b^* u_b^* + \beta - \frac{\gamma}{h^*} \tag{11}$$

with the dimensionless parameters

$$\alpha = \frac{\rho_i L_f}{[t][\tau_d][u_b]} \tag{12}$$

$$\beta = \frac{G}{[\tau_d][u_b]} = \frac{G}{a_c \rho_i g [h]} \tag{13}$$

$$\gamma = \frac{k_i \Delta T}{[h][\tau_d][u_b]} = \frac{k_i \Delta T}{a_c \rho_i g [h]^2}, \tag{14}$$

where α is the ratio of bed relaxation rate (associated with the timescale on which till water content responds to changes in the basal heat budget) to frictional heating rate, β is the ratio of geothermal heating to frictional heating, and γ is the ratio of vertical heat conduction to frictional heating. The characteristic ice thickness scale,

$$[h] = L \left[\frac{4^n (n+1) a_c}{A_g W^{n+1} (\rho_i g)^n} \right]^{\frac{1}{n+1}}, \tag{15}$$

is expressed as a fraction of ice stream length determined by the ratio of accumulation rate to the maximum ice streaming velocity (for details of non-dimensionalization and other scaling parameters, see section S1 of the auxiliary material).

[34] A linear stability analysis (see section S2 of the auxiliary material) then demonstrates that the steady-streaming mode becomes unstable when

$$\beta < \left(\frac{n+1}{n} \right)^{-\frac{n}{n+1}} \gamma - \frac{\left(\frac{n+1}{n}\right)^{\frac{n}{n+1}}}{n+1}. \tag{16}$$

The instability takes the form of a subcritical Hopf bifurcation; if started near the steady-streaming solution, the ice stream will rapidly evolve away from it in a sequence of increasing oscillations. Numerically, one can trace the subsequent evolution (using the full model that includes till freeze-on) and show that the ice stream evolves into one of the binge-purge modes, although a local analysis is not sufficient for this.

[35] We can alternatively write the relationship between geothermal heat flux (G) and surface temperature departure from T_m (ΔT) that denotes the transition from the steady-streaming mode to the binge-purge mode as

$$G = \lambda \Delta T - \kappa \tag{17}$$

where

$$\lambda = \left(\frac{4}{3} \right)^{-\frac{3}{4}} \left(\frac{A_g \rho_i^3 g^3}{a_c} \right)^{\frac{1}{4}} \frac{k_i W}{4L} \tag{18}$$

$$\kappa = \left(\frac{4}{3} \right)^{\frac{3}{4}} \left(\frac{A_g \rho_i^3 g^3}{a_c} \right)^{-\frac{1}{4}} \frac{a_c \rho_i g L}{W}. \tag{19}$$

This analytically determined boundary is the rightmost white solid line on Figure 2, confirming that the stability analysis and minor approximations therein provide a good fit to the boundary predicted by numerical simulation and our understanding of the related physical mechanisms.

3.2. Mode Transitions and Hysteresis

[36] The nature of the transition between steady-streaming and binge-purge modes is important for understanding how ice streams respond to external forcing. In this simple model, forcing may come from changes in geothermal heat flux (on geologic time scale) or changes in climate (surface ice temperature or accumulation rate). Geothermal heating is approximately constant on the time scale of a particular continental ice sheet configuration. However, surface air temperature and accumulation may plausibly change during glacial cycles or due to decadal to millennial-scale climate variability (e.g., Dansgaard-Oeschger events).

[37] We have already shown that the steady-streaming solution will become unstable when either surface temperature or geothermal heat flux is decreased (more generally, when β is decreased or γ is increased). It can be shown analytically that the transition to instability is a Hopf

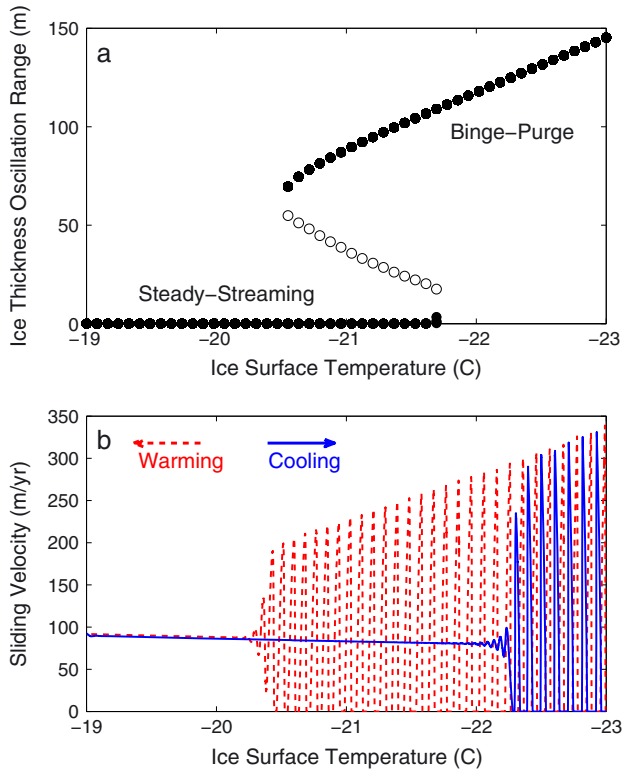

Figure 4. (a) Bifurcation diagram. Each point represents a fixed point or limit cycle determined from simulations with a single prescribed ice surface temperature and numerous initial ice thicknesses (initial till water content was kept constant near the fixed point value). Filled points are stable. Open points are unstable. (b) Transient numerical simulation with slow (0.005°C/century) increase (red) and decrease (blue) in surface ice temperature. Both panels for prescribed geothermal heat flux of 0.07 $\frac{W}{m^2}$.

bifurcation, associated with the onset of unstable oscillatory behavior. Figure 4a shows this Hopf bifurcation to be subcritical. This figure is generated by initializing the ice stream at a range of initial conditions for each distinct set of prescribed parameters (here only surface temperature is varied) and then determining if all initial conditions lead to a single final state (stable fixed point or limit cycle; filled points) or multiple final states (unstable limit cycle; open points).

[38] Further normal form transformation and analysis strongly suggest that the bifurcation is subcritical for a wide range of values for α, β and γ (see section S3 of auxiliary material). As indicated in Figure 2, the region of parameter space corresponding to modern West Antarctic ice streams (white ellipse) is in the binge-purge parameter regime. This is consistent with observations which indicate that modern Siple Coast ice streams have periodically switched between active and stagnant states in the recent past [*Retzlaff and Bentley*, 1993; *Hulbe and Fahnestock*, 2007; *Catania et al.*, 2012]. It is also notable that modern Siple Coast ice streams appear to occupy a parameter regime that is very near the stability boundary (rightmost white solid line of Figure 2) to the steady-streaming mode and the region of hysteresis (bounded by solid white lines in Figure 2).

[39] The presence of a subcritical Hopf bifurcation [*Strogatz*, 1994] necessarily implies that by changing a parameter such as surface temperature, there would be hysteresis and irreversibility in ice stream behavior. In other words, the reverse transition from a binge-purge mode to a steady-streaming mode occurs at a higher temperature (Figure 4a) than the point at which the steady-streaming mode first becomes unstable. There is, therefore, a range of surface temperatures for which both steady-streaming or binge-purge modes are possible.

[40] Figure 4b plots ice velocity as a function of surface temperature for a transient run with very slowly changing surface temperature (such that temperature varies on time scale much longer than ice stream variability). In moving from the binge-purge mode to steady-streaming (red dashed line; surface warming) there is a jump from a finite-amplitude stable limit cycle to a fixed point. In the bifurcation diagram of Figure 4a, this jump corresponds to the oscillatory solutions disappearing abruptly below $T_s = -20.5°C$; in technical parlance, this disappearance is termed a saddle-node bifurcation of limit cycles [*Strogatz*, 1994]. Similarly, in moving back from the steady-streaming mode to binge-purge (blue solid line; surface cooling) there is a another jump. The abruptness of these transitions in Figure 4b depends on the rate of surface temperature change being sufficiently slow in comparison to the growth rate of instabilities near the bifurcation point.

[41] The transition between steady-streaming and binge-purge behavior occurs at different temperatures depending on whether the ice surface temperature is increasing (red) or decreasing (blue). This experiment demonstrates the extent to which hysteresis may result in irreversible changes in ice stream behavior over a range of several degrees of surface ice temperature. Given the apparent proximity of modern Siple Coast ice streams to the bifurcation region in parameter space, these results are potentially relevant for understanding the response of Antarctic ice streams to future climate change.

3.3. Steady-Streaming Velocity

[42] In steady-streaming mode (Figures 1a and 1b), drainage and friction mediate the equilibrium sliding velocity attained by the ice stream. Steady-streaming with drainage occurs when $\beta > \gamma$ (white dashed line of Figure 2), implying that geothermal heat flux exceeds characteristic vertical heat conduction. In this case, the basal shear stress is negligibly small and the fixed point of equation (10) and $u^* = \left(\tau_d^*/h^*\right)^n$ require that $u^* = 1$; the steady-streaming velocity will be the characteristic scaled velocity, $[u_b]$. In dimensional units, the equilibrium velocity of steady-streaming with drainage,

$$u_d = W\left[\frac{A_g(\rho_i g a_c)^n}{4^n(n+1)}\right]^{\frac{1}{n+1}}, \tag{20}$$

is the velocity that would occur on an ice stream with the characteristic ice thickness (equation (15)) and a zero-strength bed.

[43] The case of steady-streaming without drainage occurs when $\gamma > \beta > \left(\frac{n+1}{n}\right)^{-\frac{n}{n+1}}\gamma - \frac{\left(\frac{n+1}{n}\right)^{\frac{n}{n+1}}}{n+1}$, implying that geothermal heat flux is less than characteristic vertical heat

conduction, and above the stability boundary. In this case, we must solve for the fixed point of (10) and (11) in the case where $\tau_b^* > 0$. (For the full analysis and higher order approximations, see section S5 of auxiliary material.) A zero-order approximation (with $n \to \infty$; accurate to within 5%) on the steady-streaming equilibrium velocity without drainage is

$$u_f = 2u_d \left[(1-\beta) + \sqrt{(\beta-1)^2 + 4\gamma} \right]^{-1}, \tag{21}$$

with β and γ defined previously. The steady-streaming velocity without drainage, u_f, is a fraction of the steady-streaming velocity with drainage, u_d. It is always the case that $u_f \leq u_d$ in the interval $\gamma > \beta > \left(\frac{n+1}{n}\right)^{-\frac{n}{n+1}} \gamma - \frac{\left(\frac{n+1}{n}\right)^{\frac{n}{n+1}}}{n+1}$.

3.4. Binge-Purge Oscillations

[44] To first order, the amplitude (Figure 2) and period (Figure 3) of the oscillations in the binge-purge mode are controlled by the ratio of vertical heat conduction to geothermal heat flux, the "ratio of equilibrium heat fluxes" (REHF). This quantity is the baseline "forcing" of the basal heat budget, which is then dynamically modified by changes in ice thickness and frictional heating. We define the REHF here as the ratio of two dimensionless parameters of the reduced model, corresponding to vertical heat conduction and geothermal heat flux,

$$\text{REHF} = \frac{\gamma}{\beta} = \frac{k_i \Delta T}{G[h]}, \tag{22}$$

where $[h]$ is the ice thickness scale. The expression $\frac{k_i \Delta T}{[h]}$ is the characteristic vertical heat conduction that would occur if ice thickness was at its characteristic scale, $[h]$. In Figures 2 and 3, a low REHF occurs in the upper left corner and high REHF in the lower right corner. The transition from steady-streaming with drainage (Figure 1a) to steady-streaming without drainage (Figure 1b) occurs on the line (dashed white line in Figure 2) where REHF is one.

[45] During stagnation, a high REHF lowers the till water content, till thickness, and basal ice temperature more than in a low REHF case. This increases the length of time that it takes the ice stream to reactivate and increases the magnitude of accumulation that occurs during the stagnant phase.

[46] Very near the stability boundary (rightmost solid white line in Figure 2) in the weak binge-purge mode, the active purge phase is a significant portion of the period of the oscillation. As REHF increases, the amplitude of the purge phase increases and the length of the purge phase decreases. This is the result of a more efficient ice stream purge caused by a strong driving stress built up during the longer binge phase.

[47] In the limit of $\alpha \ll 1$, this binge-purge mode can be thought of as a relaxation oscillation with a stagnant branch and an active purge branch, much like the glacial surge model of *Fowler* [1987]. It differs from the *Fowler* [1987] model and the canonical van der Pol oscillator [*Hinch*, 1991] in that the changes in model variables are non-smooth. Analysis of various parametric limits and the behavior of the branches in this relaxation oscillator paradigm is included in section S6 of the auxiliary material.

[48] In real ice streams, the limit of $\alpha \ll 1$ does not strictly apply, physically implying that there is a non-negligible time scale associated with bed relaxation to changes in the basal heat budget. However, a small α limit permits approximation of nullclines of the phase trajectory. These lead to approximations for the critical ice thickness at both stagnation and activation and total binge-purge period. The general strategy is to first find the critical ice thickness at stagnation, h_s, by locating the point at which the active branch of the relaxation oscillator becomes unstable (see Figure S1 in the auxiliary material). We find a second-order asymptotic approximation on this critical stagnation thickness, h_s,

$$h_s = [h] \left[\left(\frac{\gamma}{\eta}\right)^{\frac{1}{n+3}} - \frac{\beta}{n+3} (\eta^2 \gamma^{n+1})^{-\frac{1}{n+3}} - \frac{n}{2(n+3)^2} \beta^2 \left(\eta^3 \gamma^{2n+3}\right)^{-\frac{1}{n+3}} \right], \tag{23}$$

with $\eta = \frac{n^n}{(n+1)^{n+1}}$. This generally agrees with the stagnation thickness given by the ice stream model to within 5%.

[49] During the stagnant phase, the ice sliding velocity is (by definition) zero. This greatly simplifies the reduced model as thickness increases linearly with accumulation and till water content decreases to a minimum at $h = [h]\frac{\gamma}{\beta}$ (from equation (11) when $u_b = 0$) and then increases until the critical activation water content and ice thickness are reached. For parameter regimes away from the stability boundary in which the duration of stagnation is much greater than the duration of active streaming, we can derive an approximation on the total binge-purge period

$$T = \frac{\gamma}{\beta - \frac{\gamma}{2\frac{\gamma}{\beta} - h_s}} \left[\ln\left(2\frac{\gamma}{\beta h_s} - 1\right) - \frac{\frac{\gamma}{\beta} - h_s}{\frac{\gamma}{\beta} - \frac{h_s}{2}} \right] \left(\frac{[h]}{a_c}\right) \tag{24}$$

This confirms the analysis of small α that to first order, period increases with REHF. This approximation agrees with the period given by the ice stream model (Figure 3) to within 10% away from the stability boundary in the weak binge-purge parameter regime. Ignoring basal cooling during stagnation and neglecting the surge duration in our earlier approximation for h_s all contribute to this error. However, without these approximations, closed-form solutions for the binge-purge period and critical thicknesses are unattainable.

[50] This directly leads to an approximation for the critical activation thickness, h_a,

$$h_a = h_s + [h]T, \tag{25}$$

which agrees with the critical activation thickness given by the ice stream model in the weak-binge-purge mode to within 10%.

[51] The details of the derivations above and additional asymptotic analyses of the binge-purge solutions are included in section S7 of the auxiliary material.

4. Model Limitations and Future Prospects

[52] This study reduces a three-dimensional thermomechanical ice stream with hydrology to a zero-dimensional model. Without resolving streamwise variations, we have made the implicit assumption that activation and stagnation occurs simultaneously throughout the domain. In reality, the local effects of hydrology on ice dynamics will propagate at some finite time scale, which may impact if and how

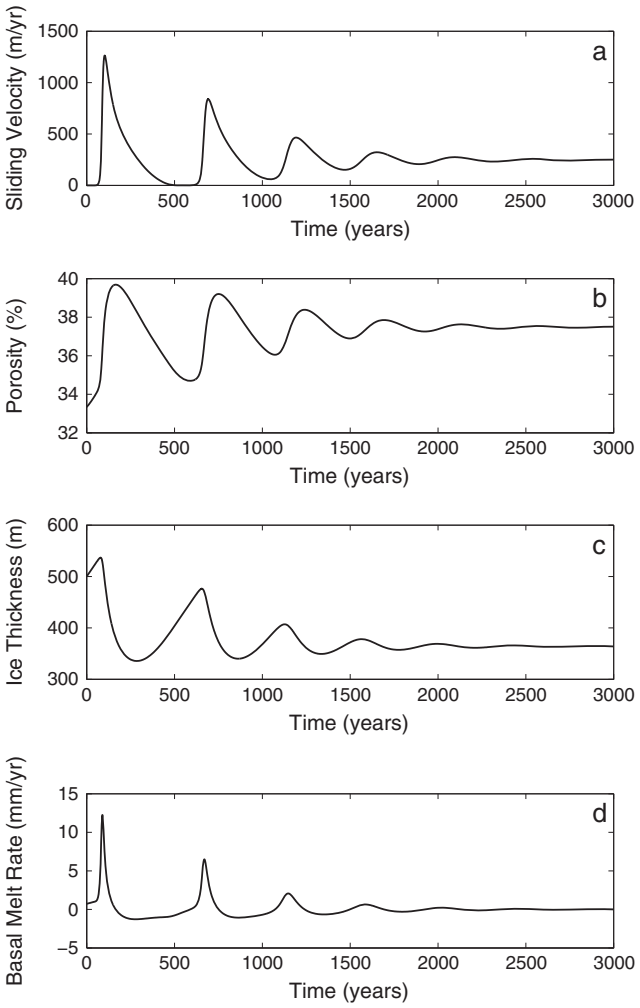

Figure 5. Simulation replicating parameter regime of experiment 1 in Figure 2 of [*Bougamont et al.*, 2011]. We used all parameters given in that study and estimate ice stream width to be 35 km and A_g to be 7×10^{-25} $Pa^{-3}s^{-1}$ (corresponding to an average temperature of –7°C in the ice stream). (a) Sliding velocity. (b) Till porosity (note that till porosity $\phi = \frac{e}{1+e}$). (c) Ice thickness. (d) Basal melt rate.

meltwater production throughout the ice stream responds to changes in ice stream thickness. Although this may change some of the details of regimes in parameter space (Figures 2 and 3), we expect that the relatively short adjustment time scale of bed relaxation (years) will still produce the modes of behavior explored in Figure 1.

[53] Similarly, we assumed the vertical temperature profile of the ice stream to be linear in order to simplify the calculation of vertical heat conduction. There are two possible justifications for this: for a stagnant ice stream, a linear temperature gradient could be the result of diffusion-dominated heat transport. For a rapidly-moving ice stream depleting previously stagnant ice on a much faster time scale, rapid advection can equally preserve the shape of the vertical temperature distribution, with the same basal and surface temperatures as before, but compressing the temperature gradient as the ice stream thins. A major limitation of our approach in either case is that temperature changes at the ice surface are propagated instantaneously to the bed. Hence, if we change the parameter T_s transiently (as in Figure 4b), we assume that this is instantly felt at the bed. In reality, the diffusion time scale for ice thicknesses of order 10^3 m can stretch to thousands of years. In addition, field measurements of the vertical temperature profile in ice streams exhibit weak temperature gradients in the upper portion of the ice thickness and much stronger temperature gradients in basal ice [*Gow et al.*, 1968; *Engelhardt and Kamb*, 1993]. Deviation of the measured temperature profile from a linear approximation is primarily the result of horizontal advection of heat in basal ice [*Joughin et al.*, 2004]. Thus, dynamically calculating a more realistic temperature profile (in the manner of *MacAyeal* [1993]) would likely result in stronger temperature gradients in basal ice and an enhancement of vertical heat fluxes at the ice-bed interface. Although this may result in a shift of the parameter regimes, it would not necessarily change the overall structure. Complex interactions between climate forcing on millennial time scales, with similar diffusive time scales and the intrinsic time scale of binge-purge oscillations may yield interesting behavior with relevance to understanding ice sheet responses to climatic variability.

[54] Previous studies of ice streams [*Bougamont et al.*, 2011; *Sayag and Tziperman*, 2011] have calculated (rather than specified) the evolution of ice stream width using complex ice dynamical models. Our prescription of ice stream width neglects the importance of ice advection across shear margins and shear margin migration during activation and stagnation [*Schoof*, 2012]. However, bedrock geometry may simply confine ice stream geometry to a fixed width,

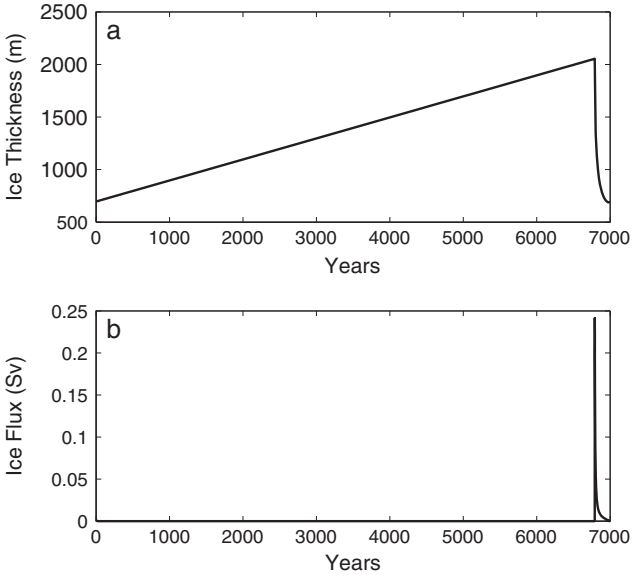

Figure 6. Heinrich event simulation with ice stream 800 km long, 90 km wide, catchment area of 1.44×10^5 km^2, 2 m thick effective till layer, geothermal heat flux of 0.05 W m^2 and ice surface temperature of T_s = –35°C. (a) Ice thickness. (b) Instantaneous ice flux in units of sverdrups. Note that "catchment area" refers to surrounding ice field with thickness the same as ice stream trunk—presumably the ice stream draws ice from a much larger region.

and this still represents a reasonable first approximation to make. In any case, prescribing ice stream width enabled the exploration of the impacts of ice stream geometry on flow variability in the above analysis.

[55] Saturation and consolidation thresholds are utilized in our model in order to include necessary physics without complicating the model. The till consolidation threshold, e_c, is the point at which ice-debris interlayering and ice lensing occur in subglacial till, preventing further extraction of water from the till and basal freeze-on of meltwater. We have set e_c = 0.3, but its exact value is uncertain [*Christoffersen and Tulaczyk*, 2003; *Rempel*, 2008]. The till saturation threshold, w_s, represents the point at which till becomes impermeable to further addition of meltwater. In the simulations presented in this study, w_s = 1 m, ensuring that saturation is reached when the bed is very weak. More observational data are necessary to determine the actual value of w_s for subglacial tills, which may affect our estimate of the steady-streaming velocity for ice streams with drainage [equation (20)].

[56] The dynamic evolution of subglacial drainage networks has been neglected in this study. Complex model studies [i.e., *van der Wel et al.*, 2013; *Bougamont et al.*, 2011] have modeled or parameterized drainage evolution beneath ice streams. The inclusion of dynamic drainage would likely have the effect of producing regional transport of meltwater within the ice stream trunk. The addition of a realistic upstream meltwater source and subglacial lakes in topographic troughs would impact the distribution of bed strength and ice stream behavior. Unfortunately, it is not feasible to realistically simulate such behavior in the present simple model.

[57] The rate of vertical heat conduction in our model depends on a single prescribed atmospheric temperature. This neglects the impact of atmospheric lapse rate on the surface ice temperature and we also ignore the temperature dependence of effective ice viscosity, which is assumed constant in this study. Similarly, our assumed constant accumulation rate neglects the dependence of precipitation on elevation. Nonetheless, this study produces binge-purge oscillations of similar period and amplitude to studies such as *MacAyeal* [1993], which includes lapse rate effects on top of a prescribed sea level atmospheric temperature. The surface elevation gradients of modern ice streams are not sufficiently large to expect that there would be a significant impact on ice surface temperature and accumulation rate. This may be different in the case of the ice stream that caused Heinrich events, which may develop large surface elevation gradients (see bottom-right corner of Figure 2 and the simulation of Figure 5).

[58] *Echelmeyer et al.* [1994] suggests that the temperature dependence of ice rheology and dynamic effects like strain heating and fabric development in ice stream shear margins may be important. Although the temperature dependence of ice rheology is known, accounting for other complex thermodynamic processes requires a sophisticated model, which is well beyond the scope of this study.

[59] The model's simplicity enabled us to easily interpret its behavior in terms of a limited set of parameters and processes. Further study with more complex models may reveal that there are other physical processes which contribute to ice stream variability. There are several ways in which this model can be improved, mainly by adding realism and eliminating simplifying assumptions.

5. Implications for Heinrich Events and Variability in Complex Models

[60] Here we explore the implications of our simple model for understanding two sets of results: (a) variability in complex ice flow models and (b) variability of a Hudson Strait ice stream as a cause for Heinrich events.

[61] Experiment one of *Bougamont et al.* [2011] coupled a 3D thermomechanical ice flow model to the undrained plastic bed model of *Tulaczyk et al.* [2000b], producing damped oscillations in ice stream flow. In Figure 5, we have utilized the parameters provided in that study, and found that the ice stream of Figure 2 of *Bougamont et al.* [2011] is in a parameter regime of our model that produces damped oscillations to a steady-streaming mode without drainage. Comparing the two models, we find that during purge phases, our modeled ice stream rapidly activates and then gradually stagnates, which is the reverse of *Bougamont et al.* [2011]. Additionally, our model reaches a steady state of moderate speed, whereas *Bougamont et al.* [2011] reverts to a slow-moving "ice sheet mode." Although our model is much simpler than that of *Bougamont et al.* [2011], we suggest that the sustained oscillations produced in experiment two of *Bougamont et al.* [2011] may be obtained by changing the model's prescribed parameters in order to bring it to the lower right region in our parameter space (Figure 2). This could replace the ad hoc drainage parameterization used in experiment two of *Bougamont et al.* [2011] in order to obtain sustained oscillatory behavior.

[62] For the purpose of comparing our simple model to Heinrich event models, we posit a hypothetical Hudson Strait Ice Stream that is 800 km long, 90 km wide (based on the Hudson Strait bathymetry given by *Andrews and Maclean*, [2003]), with a catchment area covering 25% of Hudson Bay, an effective till layer thickness of 2 meters (based on estimates of total IRD volume, see *Hemming*, [2004]), geothermal heat flux of 0.05 W m^2 and ice surface temperature of T_s = –35°C (matching the parameters used by *MacAyeal*, [1993] with all other parameters the same as elsewhere in this study, see Table 1). A simulation from our simple model in this parameter regime (Figure 6) yields a strong binge-purge oscillation with a total period of 7026 years, a purge phase duration of 208 years, total ice discharge of 1×10^5 km^3 and peak discharge of 0.24 Sv. Although these numbers are dependent on poorly constrained ice stream geometry and ice fabric parameters, they are very close to those found by *MacAyeal* [1993], who prescribed a purge time scale of 250 years and simulated a Heinrich event period of 7260 years. We conclude that a dynamically determined purge time scale is important in constructing a physically consistent portrait of the Hudson Strait ice stream.

[63] The range in total ice discharge (3×10^4 to 5×10^6 km^3), peak discharge (0.15 to 1 Sv), duration (2×10^2 to 2×10^3 years) and period (7×10^3 to 1×10^4 years) of Heinrich events provided by proxy records [*Hemming*, 2004] is large to the degree that it does not provide a strong constraint on Heinrich events. Nonetheless, this modeling exercise has demonstrated that the variability produced by both modern

Siple Coast ice streams and a Hudson Strait ice stream can be feasibly explained by the thermal mechanism explored earlier. Future study may then be able to use a more sophisticated version of this model to further constrain the Heinrich event record.

6. Conclusions

[64] We analyzed the results of a simple model of ice stream dynamics, coupling basal hydrology with ice flow and including subglacial drainage and till mechanics. This adds physics not captured in previous simple ice stream models, while retaining sufficient simplicity to enable robust analysis of model dynamics in a way not feasible with complex models.

[65] In our simple model, we find that geothermal heat flux and surface temperature control vertical basal heat budget and determine the character of the ice flow, of which we found two potential modes of behavior. A steady-streaming mode is maintained by both drainage and frictional heating at the ice-bed interface, and is qualitatively similar to the ice stream mode described in *Tulaczyk et al.* [2000b]. Unlike *Tulaczyk et al.* [2000b], the steady-streaming mode in our model depends on the dynamic ice thickness and in some cases, the development of subglacial drainage. *Sayag and Tziperman* [2009, 2011] also found a transition between streaming and oscillations using a multi-valued basal sliding law, as they varied the accumulation rate. Their model resolved the spatial structure of the ice stream, yet did not simulate the basal hydrology as in this study. The connection of the results here to such sliding laws remains an interesting question for future research.

[66] An oscillatory binge-purge mode is found here with periods ranging from hundreds to tens of thousands of years and amplitude in ice thickness ranging from tens to thousands of meters. The oscillation is primarily caused by meltwater freeze-on during stagnation due to ice thinning and the resulting strengthening of diffusive heat flux away from basal ice. The reverse process of meltwater production occurs during activation.

[67] The transition between the steady-streaming mode and the binge-purge mode is a subcritical Hopf bifurcation for a range of physically realizable parameters. Experiments where one or more physical parameters are varied across the bifurcation indicate that there is hysteresis in ice stream behavior. As a result, the ice surface temperature at which an ice stream transitions between steady and oscillating changes depending on whether the temperature increases or decreases. This is a new behavior that has not been found in previous studies of ice stream variability, with significant potential implications to our understanding of the mass balance of the Antarctic ice sheet.

[68] The ice stream variability simulated in this study is also useful for interpreting earlier, more complex, ice stream models. It is likely that one of the experiments of *Bougamont et al*. [2011] does not produce sustained oscillations in ice stream flow because it resides in the steady-streaming regime of parameter space. Furthermore, our model is able to produce ice stream variability that resembles Heinrich events in both period and amplitude, while constraining a number of characteristics of a hypothetical Hudson Strait ice stream that may be the cause of Heinrich events.

[69] **Acknowledgments.** This work has been supported by the NSF climate dynamics program, grant ATM-0902844 P2C2 (A.R. and E.T.). E.T. thanks the Weizmann Institute for its hospitality during parts of this work. A.R. has been supported by the National Defense Science and Engineering Graduate Fellowship. C.S. has been supported by NSERC Discovery Grant 357193-08. We thank the three anonymous reviewers and Ian Hewitt, Jim Rice, Marianne Haseloff, and Joe Fitzgerald for helpful conversations in the completion of this work.

References

Alley, R., D. Blankenship, C. Bentley, and S. Rooney (1986), Deformation of till beneath ice stream B, West Antarctica, *Nature*, *322*(6074), 57–59.

Andrews, J., and B. Maclean (2003), Hudson Strait ice streams: A review of stratigraphy, chronology and links with North Atlantic Heinrich events, *Boreas*, *32*(1), 4–17.

Bamber, J., D. Vaughan, and I. Joughin (2000), Widespread complex flow in the interior of the Antarctic ice sheet, *Science*, *287*(5456), 1248–1250.

Blankenship, D., C. Bentley, S. Rooney, and R. Alley (1986), Seismic measurements reveal a saturated porous layer beneath an active Antarctic ice stream, *Nature*, *322*(6074), 54–57.

Blatter, H. (1995), Velocity and stress fields in grounded glaciers—A simple algorithm for including deviatoric stress gradients, *J. Glaciol.*, *41*, 333–344.

Bougamont, M., S. Tulaczyk, and I. Joughin (2003a), Numerical investigations of the slowdown of Whillans Ice Stream, West Antarctica: Is it shutting down like Ice Stream C? *Ann. Glaciol.*, *37*(1), 239–246.

Bougamont, M., S. Tulaczyk, and I. Joughin (2003b), Response of subglacial sediments to basal freeze-on: 2. Application in numerical modeling of the recent stoppage of Ice Stream C, West Antarctica, *J. Geophys. Res.*, *108*(B4), 2223, doi:10.1029/2002JB001936.

Bougamont, M., S. Price, P. Christoffersen, and A. Payne (2011), Dynamic patterns of ice stream flow in a 3-D higher-order ice sheet model with plastic bed and simplified hydrology, *J. Geophys. Res. Earth Surf.*, *116*, F04018, doi:10.1029/2011JF002025.

Calov, R., et al. (2010), Results from the Ice-Sheet Model Intercomparison Project—Heinrich Event INtercOmparison (ISMIP HEINO), *J. Glaciol.*, *56*(197), 371–383.

Calov, R., A. Ganapolski, V. Petoukhov, M. Claussen, and R. Greve (2002), Large-scale instabilities of the Laurentide ice sheet simulated in a fully coupled climate-system model, *Geophys. Res. Lett.*, *29*(24), 2216, doi:10.1029/2002GL016078.

Catania, G., C. Hulbe, H. Conway, T. Scambos, and C. Raymond (2012), Variability in the mass flux of the Ross ice streams, West Antarctica, over the last millennium, *J. Glaciol.*, *58*(210), 741–752.

Christoffersen, P., and S. Tulaczyk (2003), Response of subglacial sediments to basal freeze-on 1. Theory and comparison to observations from beneath the West Antarctic Ice Sheet, *J. Geophys. Res.*, *108*(B4), 2222, doi:10.1029/2002JB001935.

Dunse, T., R. Greve, T. Schuler, and J. Hagen (2011), Permanent fast flow versus cyclic surge behaviour: Numerical simulations of the Austfonna ice cap, Svalbard, *J. Glaciol.*, *57*(202), 247–259.

Echelmeyer, K., W. Harrison, C. Larsen, and J. Mitchell (1994), The role of the margins in the dynamics of an active ice stream, *J. Glaciol.*, *40*, 527–538.

Engelhardt, H., and B. Kamb (1993), Vertical temperature profile of Ice Stream B, *Antarct. J. US*, *28*(5), 63–66.

Engelhardt, H., and B. Kamb (1997), Basal hydraulic system of a West Antarctic ice stream: Constraints from borehole observations, *J. Glaciol.*, *43*(144), 207–230.

Engelhardt, H., N. Humphrey, B. Kamb, and M. Fahnestock (1990), Physical conditions at the base of a fast moving Antarctic ice stream, *Science*, *248*(4951), 57–59.

Fowler, A. (1987), A theory of glacial surges, *J. Geophys. Res.*, *92*(B9), 9111–9120, doi:10.1029/JB092iB09p09111.

Fowler, A., T. Murray, and F. Ng (2001), Thermally controlled glacier surging, *J. Glaciol.*, *47*(159), 527–538.

Gow, A., H. Ueda, and D. Garfield (1968), Antarctic ice sheet: Preliminary results of first core hole to bedrock, *Science*, *161*(3845), 1011–1013.

Heinrich, H. (1988), Origin and consequences of cyclic ice rafting in the Northeast Atlantic Ocean during the past 130,000 years, *Quat. Res.*, *29*, 142–152.

Hemming, S. R. (2004), Heinrich events Massive late pleistocene detritus layers of the North Atlantic and their global climate imprint, *Rev. Geophys.*, *42*(1), 1–43.

Herterich, K. (1987), On the flow within the transition zone between ice sheet and ice shelf, in *Dynamics of the West Antarctic Ice Sheet. Proceedings of a Workshop Held in Utrecht, May 6–8, 1985*, edited by C. van der Veen and J. Oerlemans, pp. 185–202, D. Reidel, Dordrecht.

Hinch, E. (1991), *Perturbation Methods*, pp. 116–120, Cambridge Univ. Press, Cambridge, UK.

Hulbe, C., and M. Fahnestock (2007), Century-scale discharge stagnation and reactivation of the Ross ice streams, West Antarctica, *J. Geophys. Res. Earth Surf.*, *112*, F03S27, doi:10.1029/2006JF000603.

Hulbe, C., and I. Whillans (1997), Weak bands within, Ice Stream B, West Antarctica, *J. Glaciol.*, *43*(145), 377–386.

Jackson, M., and B. Kamb (1997), The marginal shear stress of Ice Stream B, West Antarctica, *J. Glaciol.*, *43*, 415–426.

Joughin, I., and S. Tulaczyk (2002), Positive mass balance of the Ross ice stream, West Antarctica, *Science*, *295*, 476–452.

Joughin, I., S. Tulaczyk, D. MacAyeal, and H. Engelhardt (2004), Melting and freezing beneath the Ross ice streams, Antarctica, *J. Glaciol.*, *50*(168), 96–108, doi:10.3189/172756504781830295.

Lingle, C., and T. Brown (1987), A subglacial aquifer bed model and water pressure dependent basal sliding relationship for a West Antarctic ice stream, in *Dynamics of the West Antarctic Ice Sheet*, edited by C. van der Veen, J. Oerlemans, and D. Reidel, pp. 249–285, Dordrecht, Netherlands.

MacAyeal, D. (1993), Binge/purge oscillations of the Laurentide ice sheet as a cause of the North Atlantic Heinrich events, *Paleoceanography*, *8*(6), 775–784.

Marshall, S. J., and G. K. C. Clarke (1997), A continuum mixture model of ice stream thermomechanics in the Laurentide ice sheet 2. Application to the Hudson Strait Ice Stream, *J. Geophys. Res.*, *102*(B9), 20,615–20,637

Pattyn, F. (2002), Transient glacier response with a higher-order numerical ice-flow model, *J. Glaciol.*, *48*, 467–477.

Payne, A. (1995), Limit cycles in the basal thermal regime of ice sheets, *J. Geophys. Res.*, *100*(B3), 4249–4263.

Raymond, C. (1996), Shear margins in glaciers and ice sheets, *J. Glaciol.*, *42*(140), 90–102.

Raymond, C. (2000), Energy balance of ice streams, *J. Glaciol.*, *46*(155), 665–674.

Rempel, A. (2008), A theory for ice-till interaction and sediment entrainment beneath glaciers, *J. Geophys. Res.*, *113*, F01013, doi:10.1029/2007JF000870.

Retzlaff, R., and C. Bentley (1993), Timing of stagnation of Ice Stream C, West Antarctica, from short pulse radar studies of buried surface crevasses, *J. Glaciol.*, *39*(133), 553–561.

Sayag, R., and E. Tziperman (2009), Spatiotemporal dynamics of ice streams due to a triple valued sliding law, *J. Fluid Mech.*, *640*, 483–505, doi:10.1017/S0022112009991406.

Sayag, R., and E. Tziperman (2011), Interaction and variability patterns of ice streams under a triple-valued sliding law and a non-Newtonian rheology, *J. Geophys. Res.*, *116*, F01009, doi:10.1029/2010JF001839.

Schoof, C. (2006), A variational approach to ice stream flow, *J. Fluid Mech.*, *556*, 227–251, doi:10.1017/S0022112006009591.

Schoof, C. (2010), Ice-sheet acceleration driven by melt supply variability, *Nature*, *468*(7325), 803–806, doi:10.1038/nature09618.

Schoof, C. (2012), Thermally driven migration of ice stream shear margins, *J. Fluid Mech.*, *712*, 552–578.

Strogatz, S. (1994), *Nonlinear Dynamics and Chaos*, pp. 241–284, Westview Press, Cambridge, Mass.

Tulaczyk, S., W. Kamb, and H. Engelhardt (2000a), Basal mechanics of Ice Stream B, West Antarctica 1. Till mechanics, *J. Geophys. Res.*, *105*(B1), 463–481, doi:10.1029/1999JB900329.

Tulaczyk, S., W. Kamb, and H. Engelhardt (2000b), Basal mechanics of Ice Stream B, West Antarctica 2. Undrained plastic bed model, *J. Geophys. Res.*, *105*(B1), 483–494, doi:10.1029/1999JB900328.

van der Veen, C., and I. Whillans (1996), Model experiments on the evolution and stability of ice streams, *Ann. Glaciol.*, *232*, 129–137.

van der Wel, N., P. Christoffersen, and M. Bougamont (2013), The influence of subglacial hydrology on the flow of Kamb Ice Stream, West Antarctica, *J. Geophys. Res.*, *118*, 1–14, doi:10.1029/2012JF002570.

Van Pelt, W., and J. Oerlemans (2012), Numerical simulations of cyclic behaviour in the Parallel Ice Sheet Model (PISM), *J. Glaciol.*, *58*(208), 347–360.

Vogel, S., S. Tulaczyk, B. Kamb, H. Engelhardt, F. Carsey, A. Behar, A. Lane, and I. Joughin (2005), Subglacial conditions during and after stoppage of an Antarctic Ice Stream: Is reactivation imminent? *Geophys. Res. Lett.*, *32*, L14502, doi:10.1029/2005GL022563.

Winberry, J., S. Anandakrishnan, and R. Alley (2009), Seismic observations of transient subglacial water-flow beneath MacAyeal Ice Stream, West Antarctica, *Geophys. Res. Lett.*, *36*, L11502, doi:10.1029/2009GL037730.